Large Format Quantum Well Infrared Photodetector Arrays for Astronomical Instrumentation

Sumith Bandara, Sarath Gunapala, James Bock, Michael Ressler, John Liu, Edward Luong, and Michael Werner.

Jet Propulsion Laboratory
California Institute of Technology
4800, Oak Grove Drive
Pasadena, CA 91109

Abstract

Quantum Well Infrared Photodetectors (QWIPs) afford greater flexibility than the usual extrinsically doped semiconductor IR detectors. The wavelength of the peak response and cutoff can be continuously tailored over a range wide enough to enable light detection at any wavelength range between 6-20 μm. The spectral band width of these detectors can be tuned from narrow ($\Delta\lambda/\lambda$ ~ 10 %) to wide ($\Delta\lambda/\lambda$ ~ 40 %) allowing various applications. Also, QWIP device parameters can be optimized to achieve extremely high performances at lower operating temperatures (~ 30 K) due to exponential suppression of dark current. Furthermore, QWIPs offer low cost per pixel and highly uniform large format focal plane arrays (FPAs) mainly due to mature GaAs/AlGaAs growth and processing technologies. The other advantages of GaAs/AlGaAs based QWIPs are higher yield, lower 1/f noise and radiation hardness. Recently, we operated an infrared camera with a 256x256 QWIP array sensitive at 8.5 μm at the prime focus of the 5-m Hale telescope, obtaining the images. The remarkable noise stability – and low 1/f noise – of QWIP focal plane arrays enable camera to operate by modulating the optical signal with a nod period up to 100 s. A 500 s observation on dark sky renders a flat image with little indication of the low spatial frequency structures associated with imperfect sky subtraction or detector drifts.

Spectral coverage of conventional interband infrared (IR) detectors are entirely determined by the bandgap because photoexcitation occurs across the band gap (E_g) from the valence to conduction band. Therefore, detection of mid wavelength (8-15 μm) IR radiation requires small bandgap materials such as $Hg_{1-x}Cd_xTe$ and $Pb_{1-x}Sn_xTe$, in which the energy gap can be controlled by varying x. It is well known that these low band gap materials are more difficult to grow and process than large band gap semiconductors such as GaAs. Thus, it is extremely difficult to produce them in large format uniform arrays. Quantum Well Infrared Photodetectors (QWIPs) avoid such difficulties because they are fabricated using high bandgap materials systems such as $GaAs/Al_xGa_{1-x}As$ [1-4]. It can provide highly uniform, large format focal plane array at lower cost enabling observation covering large areas. Cameras utilizing QWIP FPAs as large as 640 x 486 format arrays have been demonstrated with corrected uniformity better than 99.95% [3,4]. Due to use of artificially created band structure, spectral band width of these detectors can be tailored from narrow ($\Delta\lambda/\lambda \sim 10$ %) to wide ($\Delta\lambda/\lambda \sim 50$ %) in the wavelength range between 4-20 μm allowing various applications [5]. In addition, recent demonstration of the simultaneously readable, dual band, 640x486 QWIP FPA will provide innovative ways of simplify IR sensing instruments [6].

I. QWIP Operating Principle:

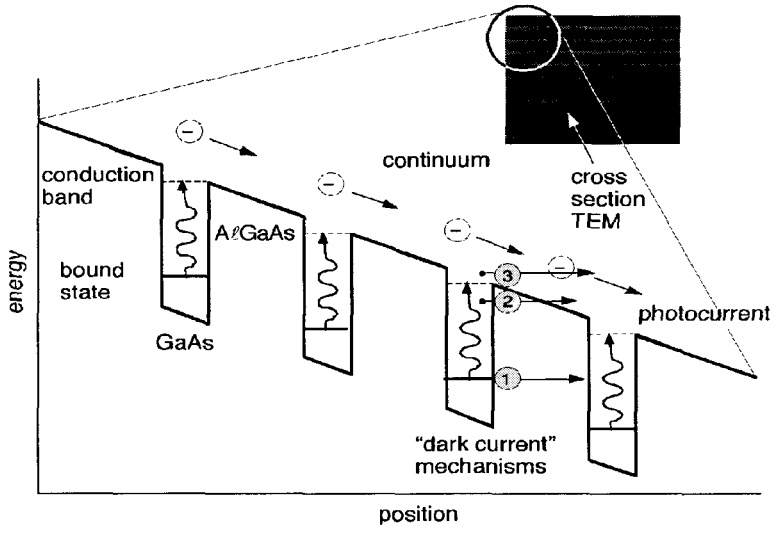

Fig 1 Schematic diagram of the conduction band in a bound-to-quasibound QWIP in an externally applied electric field. Absorption of IR photons can photoexcite electrons from the ground state of the quantum well into the continuum, causing a photocurrent. Three dark current mechanisms are also shown: ground state tunneling (1); thermally assisted tunneling (2); and thermionic emission (3).

QWIPs operate by photoexcitation of electrons between ground and first excited state subbands of multi-quantum wells (MQWs) which are artificially fabricated by placing thin layers of two different, high-bandgap semiconductor materials alternately

[1,2]. The bandgap discontinuity of two materials creates quantized subbands in the potential wells associated with conduction bands or valence bands. The structure parameters are designed so that the photo-excited carriers can escape from the potential wells and be collected as photocurrent. See Fig. 1.

The absolute responsivity R(λ) of a QWIP can be written in terms of absorption quantum efficiency ($\eta_a(\lambda)$) and photoconductive gain (g) as , $R(\lambda) = (e/h\nu)\eta_a(\lambda)g$ [1,2]. Typical absorption quantum efficiency of a QWIPs is $\eta_a(\lambda)$ ~ 10%-30%, and directly proportional to carrier doping density of the multi-quantum well structure. Photoconductive gain of a QWIP detector is determined by the position of the excited state relative to the barrier and the number of quantum wells in the structure [7,8]. For a typical 50 quantum well bound-to-quasibound QWIP, photoconductive gain g varies from ~ 10% to ~ 50% with the operating bias voltage. The net quantum efficiency (quantum efficiency and gain product) of a QWIP is reduced due to less than 100% gain resulting a lower photocurrent. However, resulting signal to noise ratio do not reduced by the same factor because both dark current and noise of the detector will be reduced due to the same reason. Also, it is important to note that, background-limited sensitivity is *independent* of photoconductive gain g.

II Spectral Tunability

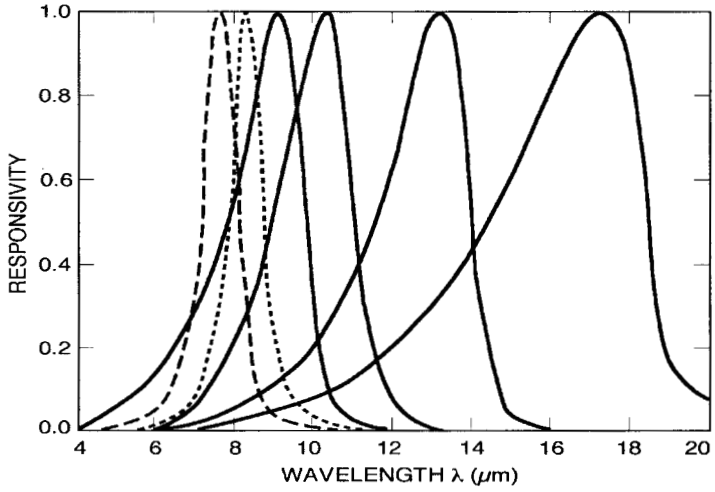

Fig 2

Fig. 2 . *This figure shows the spectral coverage and tailorability of QWIPs in 4-20 μm wavelength range.*

The lattice matched GaAs/$Al_xGa_{1-x}As$ material system is commonly used to create a QWIP structures similar to the one shown in Figure 1. Highly uniform and pure crystal layers of such semiconductors can be grown on large substrate wafers, with control of each layer thickness down to a fraction of a molecular layer, using modern crystal-growth methods like molecular beam epitaxy (MBE). Thus, by controlling the quantum well width and the barrier height (which depends on the Al molar ratio of

$Al_XGa_{1-X}As$ alloy), this intersubband transition energy can be varied over a wide enough range to enable light detection at any wavelength range between 4-20 μm (Fig.2) [1-5].

Spectral responsivity peak wavelength (λ_p) of a QWIP is determined by the energy difference between ground and excited states of the quantum well. Unlike the responsivity spectra of intrinsic infrared detectors, QWIPs spectra are much narrower and sharper due to their resonance intersubband absorption. Typically, responsivity spectra of the *bound* and *quasibound* excited state QWIPs are much narrower ($\Delta\lambda/\lambda \sim 10\%$) than the *continuum* QWIPs ($\Delta\lambda/\lambda = 24\ \%$) [1,2]. This is due to the fact that, when the excited state is placed in the continuum band above the barrier, the energy width associated with the state becomes wide. Spectral band width of these QWIPs can be further increased by replacing single quantum wells with small superlattice structures (several quantum wells separated by thin barriers) in the multi-quantum well structure [5]. Such a scheme creates an excited state miniband due to overlap of the excited state wavefunctions of quantum wells. Energy band calculations based on a two band model shows excited state energy levels spreading greater than 30 meV [5]. Figure 3 shows experimentally measured responsivity spectra with 50% bandwidth $\Delta\lambda > 5$ μm [5]. See Fig. 4. Thus, control of the processing allows us to tailor the QWIP characteristics to the specific application in hand.

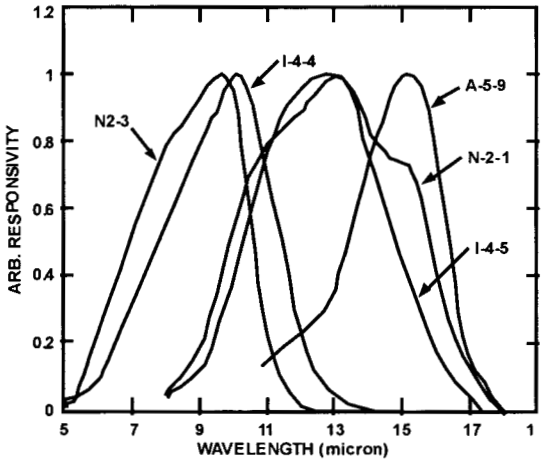

Figure 3. Spectral responsivity of several broad-band QWIPs which shows spectral coverage and tailorability of QWIPs in 4-20 μm wavelength range.

III. QWIP FPAs for Ground base Astronomy

One can improve the absorption quantum efficiency by adding more carriers into the quantum wells [1,2]. However, carrier density cannot be increased boundlessly because it leads to a higher dark current, which degrades the performance of the detector. The dominant noise in QWIP devices is due to the shot noise resulting from the dark current in the device [2,7,8]. Therefore, it is required to find the optimum N_D within the given constrains of the application. As shown in the Figure 1, the dark current originates

from three main processes; well to well quantum mechanical tunneling, thermally assisted tunneling, and classical thermionic emission. Consequently, for QWIPs operating at higher temperatures, the last mechanism is the major source of dark current. The classical thermionic emission, which can be expressed as $I_t \propto e^{-\Delta E/kT}$,where ΔE is the effective barrier height measured from the ground state Fermi level, and T is the operating temperature, decreases exponentially with decreasing operating temperature. If a detector operates at lower temperature, one can improve the photosignal of the detector by adding more carriers to the multi-quantum well structure, regardless of any increase in dark current [9]. Similar results can be achieved by designing the multi-quantum well structure to be operated in boun-to-continum mode. We have taken the advantage of both these schemes to design high sensitive QWIPs FPAs for ground base astronomical camera which operates at 30 K.

Two high performance QWIP focal plane arrays have been designed for ground-based mid-infrared camera QWICPIC (QWIP Wide-field Imaging multi-Color Prime-focus Infrared Camera) operated at the prime focus of the 5-m Hale telescope at Mt. Palomar [10]. QWIPIC is specifically designed to take advantage of the large format, narrow band, low 1/f noise, and excellent linearity and noise performance of QWIP arrays under high background conditions. This prime focus camera is designed to image a large 2' x 2' field simultaneously onto three large format focal plane arrays. QWICPIC currently houses dichroic optics enabling observations with 3 focal plane arrays simultaneously at 4.7, 8.5, and 12.5μm. The optics was designed to simultaneously optimized the image quality at the focal plane and the image quality of the pupil stop on the primary mirror. The FPAs are thermally isolated to operate at ~ 30 K.

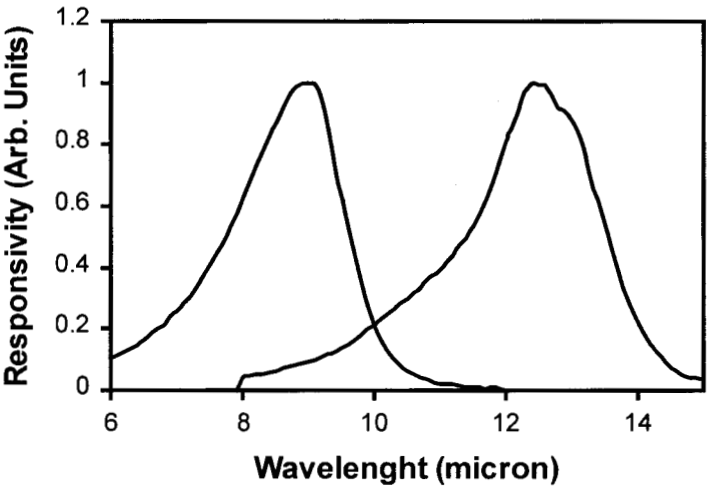

Figure 4: Spectral responsivity of two QWIP FPAs design for QWIPIC camera operated at the prime focus of the 5-m Hale telescope at Mt. Palomar.

The QWIP FPA device structures consist of 30 quantum well periods, each period containing a GaAs well and a $Al_xGa_{1-x}As$ barrier, sandwiched between top and bottom contact layers doped n = $5x10^{17}$ cm^{-3}, grown on a semi-insulating GaAs substrate. The cap layer on top of a stop-etch layer was grown *in situ* on top of the device structure to fabricate the light coupling 2-D grating structure [3,4]. The GaAs quantum well thickness and Al concentration (x) of $Al_xGa_{1-x}As$ barriers of the two devices were optimized to respond in 8-9 and 12 –13 μm spectral bands while operating in bound-to-continuum mode. Figure 4 shows the measured responsivity spectrum of each detector. Due to lower operating temperatures, dark currents were suppressed and both devices operate above back ground limited conditions. Figure 5 shows the peak responsivity vs bias voltage dependence for both devices. These responsivities show about six fold enhancement over previously demonstrated FPAs which were designed for higher operating temperatures [3].

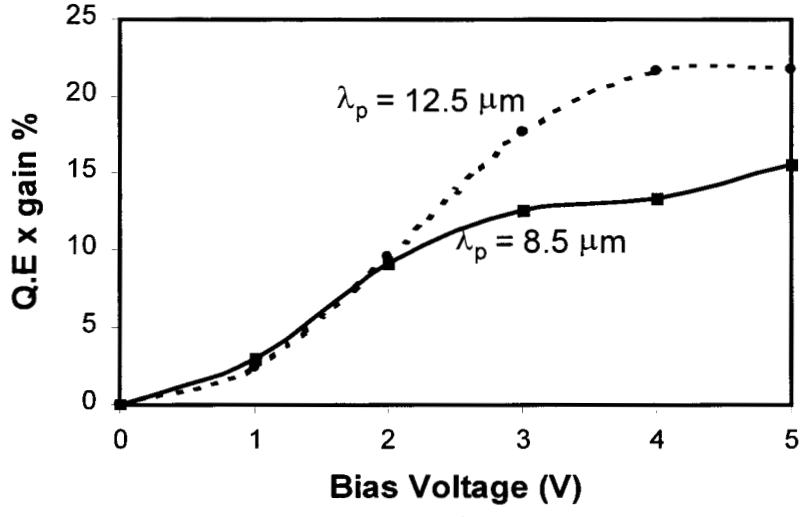

Figure 5: Quantum efficiency and gain product measured at the peak wavelengths of the high-sensitivity QWIP FPAs designed for QWIPIC camera.

First science grade 256 x 256 focal plane array was developed using the 8-9 μm QWIP wafer described in the previous paragraph and implemented in the QWICPIC camera. The excellent photometric and noise characteristics of the 256 x 256 QWIP focal plane array allow QWICPIC to observe at the prime focus of the 5-m Hale telescope. As shown in Fig. 6, the lack of 1/f noise above 10 mHz allows for slow modulation and scanning strategies commonly required in space-borne applications. The images shown

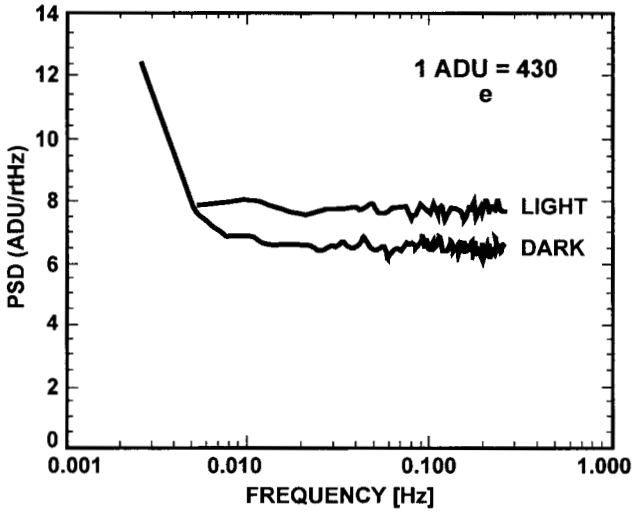

Fig.6: Noise spectral density of a 8-9 um 256 x 256 QWIP focal plane array (1 ADU = 430 e^-). The lack of 1/f noise above 10 mHz allows for slow modulation and scanning strategies commonly required in space-borne applications. QWICPIC exploits this advantage in operating at the prime focus by modulating the optical signal with a slow nod period of 20 – 100 s.

in Fig. 7 were obtained with minimal data processing: coaddition of frames, sky subtraction, removal of hot pixels, and smoothing in the case of NGC 1068. Faint structures, 10^4 times fainter than the brightest source, are apparent with no noticeable bleeding of bright sources or other non-photometric effects. The faint ring around NGC 1068 was imaged in 2400 s at a sensitivity of 3 mJy in a 1" beam. The remarkable noise stability – and low 1/f noise – of QWIP focal plane arrays enable QWICPIC to operate by modulating the optical signal with a nod period up to 100 s (see Fig.3). A 500 s observation on dark sky renders a flat image with little indication of the low spatial frequency structures associated with imperfect sky subtraction or detector drifts. To our knowledge, QWICPIC represents both the first 256 x 256 mid-infrared imager and the first successful example of a ground-based instrument using slow-nod modulation at mid-infrared wavelengths. We operate QWICPIC at the Palomar telescope without the high frequency background subtraction usually implemented for thermal infrared astronomy via a chopping secondary mirror. Instead, the subtraction was carried out at low frequency by nodding the telescope once per 30 seconds over an angle of ~5 arcmin. The resulting high quality image reflects the excellent low frequency noise performance of this device (Fig. 6). This could be a valuable attribute in an Explorer-class mission or NGST for which fiscal constraints might mitigate against either a chopping/scanning mirror or a particularly agile attitude control system. To our knowledge, QWICPIC represents both the first 256 x 256 mid-infrared imager and the first successful example of a ground-based instrument using slow-nod modulation at mid-infrared wavelengths.

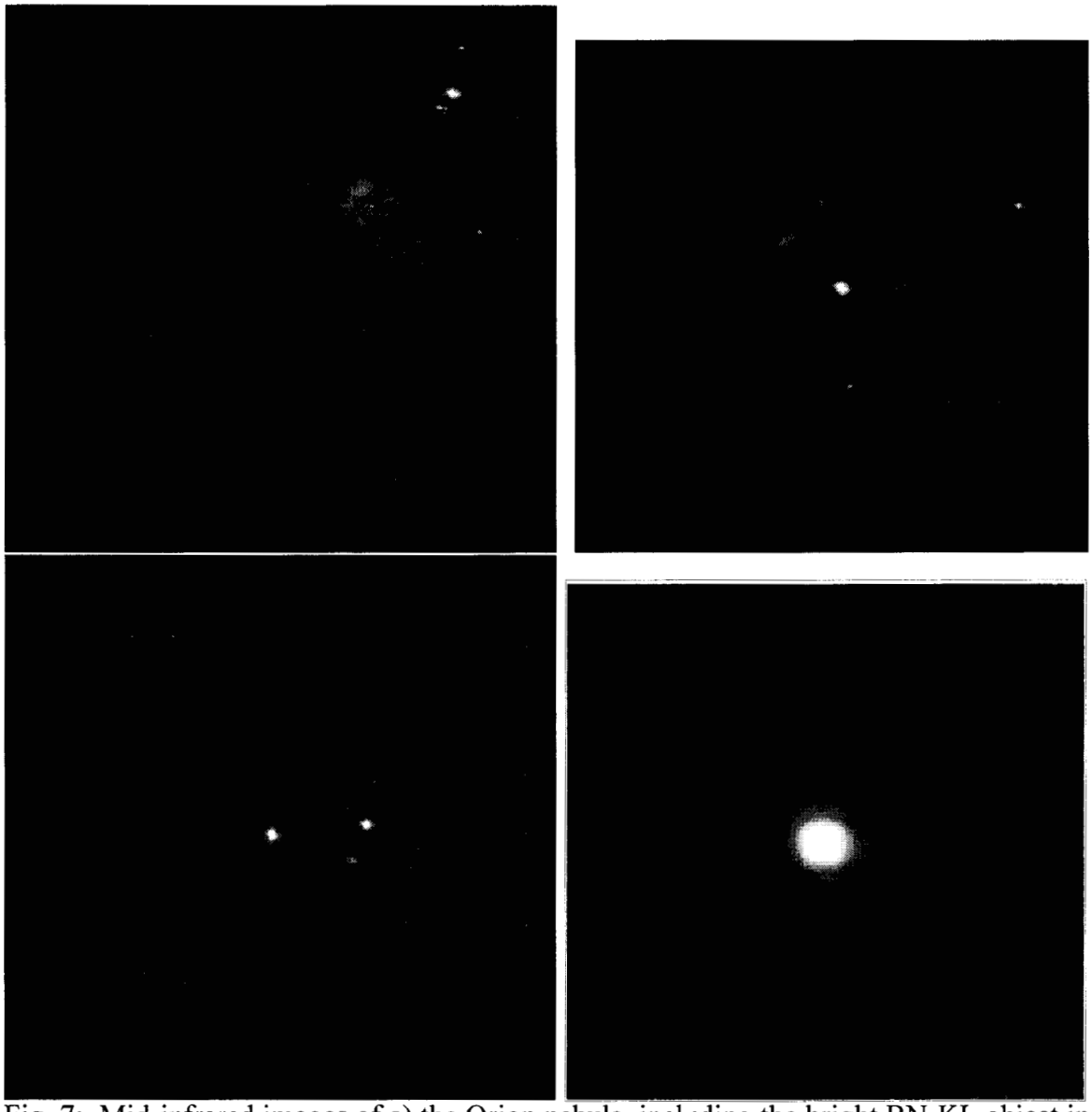

Fig. 7: Mid-infrared images of a) the Orion nebula, including the bright BN-KL object in the upper right-hand corner, the Trapezium cluster and nebula, and a shock front in the lower left-hand corner b) the Monoceros R2 star forming region, c) the W3 star forming region, and d) the faint infrared ring of NGC 1068. The images were obtained in a single night with QWICPIC using a 256 x 256 8.5 μm QWIP focal plane array in integration times of 550 – 2400 s on the sky with nod periods of 15 – 20 s. The data are scaled logarithmically in this display to enhance low surface brightness regions.

Acknowledgement:

The research described here was performed by the Center for Space Microelectronics Technology, Jet Propulsion Laboratory, California Institute of Technology, and was sponsored by the National Aeronautics and Space Administration, breakthrough sensor & instrument component technology thrust area of the cross enterprise technology development program.

References

[1] S. D. Gunapala and S. V. Bandara, Physics of Thin Films, edited by M. H. Francombe, and J. L. Vossen, Vol. 21, pp. 113-237, Academic Press, NY, 1995.

[2] B. F. Levine, J. Appl. Phys. **74**, R1 (1993).

[3] S. D. Gunapala, S. V. Bandara, J. K. Liu, W. Hong, M. Sundaram, P. D. Maker, R. E. Muller, R. Carralejo, and C. A. Shott, IEEE Trans. Elec. Devices **45**, 1890 (1998).

[4] S. D. Gunapala and S. V. Bandara, Quantum Well Infrared Photodetector (QWIP) Focal Plane Arrays, *Semiconductors and Semimetals*, 62, 197-282, Academic Press. 1999.

[5] S. V. Bandara, et al. "10-16 μm Broadband Quantum Well Infrared Photodetector", Appl. Phys. Lett., **72**, 2427 (1998).

[6] S. Gunapala, S. Bandara, A. Singh, J. Liu, S. Rafol, E. Luong, J. Mumolo, N. Tran, J. Vincent, C. Shott, J. Long, and P. LeVan. 8-9 and 14-15 μm Two-color 640x486 GaAs/AlGaAs Quantum Well Infrared Photodetector (QWIP) Focal Plane Array Camera, *SPIE* 3698, 687. 1999.

[7] K. K. Choi, J. Appl. Phys. **80**, 1257 (1996).

[8] H. C. Liu, Appl. Phys. Lett. **61**, 2703 (1992).

[9] S. D. Gunapala, S. V. Bandara, A. Singh, J. K. Liu, E. M. Luong, J. M. Mumolo, M. J. McKelvey, Proc. SPIE, v.3379, 225 (1998).

[10] M.W.Werner, et al. Paper 14.03 at San Diego AAS Meeting, 1998.